28435 DUP.

IGM88TC-402-444-G
ENRC 28435

SPIE's International Symposium and Exhibition on
Fiber Optics, Optoelectronics, and Laser Applications
in Science and Engineering
6-10 September 1988
Boston Marriott Copley Place Hotel
Boston, Massachusetts USA

BACKWARD COLLINEAR ACOUSTO-OPTIC INTERACTIONS

C.K. Jen and J.E.B. Oliveira*

Industrial Materials Research Inst., National Research Council of Canada
Boucherville, Quebec, Canada J4B 6Y4

* CTA-ITA-IEEC, 12225 Sao Jose Dos Campos, Sao Paulo, Brazil

ABSTRACT

Theoretical studies of backward collinear acousto-optic interactions (BCAOI) in bulk single crystals and single mode glass fibers are described. At very high acoustic frequencies the acoustic wavenumber k_a of the guided acoustic waves can be twice of the optical wavenumber k_o of the guided optical modes. Thus the incident optical mode propagating in the forward direction is coupled to that in the backward direction due to the index grating induced by the guided acoustic mode propagating in the collinear direction if $k_a = 2 k_o$. High efficiency is achieved due to excellent matching between profiles of the electromagnetic fields of incident, diffracted optical beam and the acoustic displacement as well as long interaction length. On- and off- line fiber optic signal processing devices such as frequency shifters, tunable filters, switches and modulators may be built using such BCAOI. Practical considerations for these devices are discussed.

1. INTRODUCTION

Acousto-optic interactions in both isotropic and anisotropic materials have been reported by many researchers [1-4]. These interactions can take place when the wavevectors of optical and acoustic waves are either collinear or noncollinear. In isotropic materials interactions in which the incident optical wave and acoustic wave are collinear and propagate in the same direction are forbidden whereas in anisotropic materials such interactions are allowed provided that the incident and diffracted optical waves have different polarizations. Those configurations in which the wavevectors are collinear and the optical waves propagate in opposite directions are, here, called backward collinear acousto-optic interaction (BCAOI). BCAOI can take place in either isotropic or anisotropic crystals. As a result of the recent advent of efficient high frequency piezoelectric transducers [5,6] BCAOI has become attractive for devices applications.

Furthermore BCAOI can also exist in single mode optical fibers. A single optical mode and a few acoustic modes are simultaneously guided in the fiber core of a cladded fiber. At very high acoustic frequency acoustic wavenumber of guided acoustic modes can be twice of the optical wavenumber of the guided optical mode. Thus the incident single optical HE_{11} mode propagating in the forward direction is coupled to that in the backward direction due to the index grating induced by the guided acoustic modes. The high efficiency is achieved due to the perfect matching of electromagnetic fields for the forward and backward propagating optical waves and a long interaction length along the fiber. The coupling coefficient of BCAOI in a single mode optical fiber using guide longitudinal types of acoustic waves will be given. Practical considerations are also discussed.

2. BCAOI IN BULK MATERIALS

In a BCAOI an acoustic wave with wavevector $\vec{k}_a$ and frequency f_a interacts with an incident optical wave with wavevector $\vec{k}_{oi}$ and frequency Ω_{oi} and gives rise to an optical wave with wavevector $\vec{k}_{od}$ and frequency Ω_{od} as illustrated in Figure 1. In such interactions conservations of momentum (wavevector) and energy (frequency) leads to the following relationships

$$\vec{k}_{oi} \pm \vec{k}_a = \vec{k}_{od} \qquad (1)$$

and

$$\Omega_{oi} \pm f_a = \Omega_{od} \qquad (2)$$

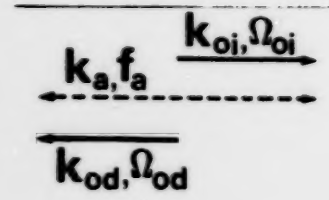

Fig.1 BCAOI

respectively. Equation (1) can be satisfied in practical devices because of the advent of the efficient high frequency piezoelectric transducers (e.g. > 10 GHz) [5,6], which allow k_a values to be higher than that of the optical wavevector k_{oi}. So far only high frequency longitudinal transducers have been reported experimentally, however in theory high frequency shear transducers may be obtainable [7].

In order to evaluate the diffraction efficiency of BCAOI let us consider the geometry shown in Fig.2; both the incident optical waves and acoustic wave propagate along the Z axis. Using the formulation presented in Ref.[8] it can be shown that when equations (1) and (2) are satisfied, the ratio between the intensities of the diffracted (I_d) and incident (I_i) optical waves at the optical entrance face, z = 0, is given by the following expression,

$$I_d/I_i = \tanh^2(CL) \qquad (3)$$

where

$$C^2 = \frac{\pi^2}{2\lambda_o} M \left(\frac{P_a}{WH}\right) \qquad (4)$$

$$M = \frac{n_i^3 n_d^3 (p_{eff})^2}{\rho v_a^3} \qquad (5)$$

n_i, n_d : refractive index of the incident and diffracted waves; ρ : material density; p_{eff} : effective photoelastic constant, P_a : acoustic power, v_a : acoustic wave phase velocity; W : acoustic transducer width; H : acoustic transducer height; λ_o : optical wavelength in vacuum; L : collinear interaction length; M: acousto-optic figure of merit.

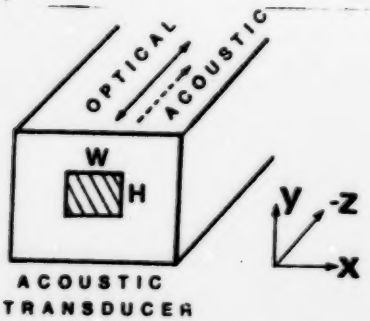

Fig.2 BCAOI configuration with acoustic transducer

2.1 ACOUSO-OPTIC FIGURE OF MERIT

As shown by Eqns.(3) and (4) when the acousto-optic figure of merit, M, is very large, high diffraction efficiency can be obtained with a low acoustic power, P_a, even with a short collinear interaction length, L. Since this is the condition under which an acousto-optic device should operate, we shall analyze M for a few materials; their relevant properties are given in Table 1.

Table 1 ACOUSTIC AND OPTICAL PROPERTIES OF MATERIALS [9]

Material	V_L (m/s)	α	n_o	n_e
Fused Silica	5933	12	1.458	1.458
Ge [1 0 0]	4924	30	4.00	4.00
$LiNbO_3$ [1 0 0]	6572	0.15	2.300	2.208
Quartz [0 0 1]	6354	2.1	1.544	1.553
TeO_2 [0 0 1]	3049	15	2.2585	2.4112

(α in db/cm-GHz^2)

2.1.1 Optical Isotropic Materials

Fused silica (FS) and germanium (Ge) are chosen because fused silica is a well known low loss isotropic material both optically and acoustically, and Ge which is optically isotropic but acoustically anisotropic exhibits very low optical loss at 10.6 μm CO_2 laser wavelength. Longer optical wavelength implies that the acoustic frequency required for BCAOI is lower, thus less acoustic attenuation. It can be shown that in isotropic materials the effective photoelastic constants, p_{eff}, is zero for BCAOI which involve pure shear acoustic waves, thus BCAOI involving shear waves are forbidden. For BCAOI in optically isotropic materials involving longitudinal acoustic waves there is no rotation of the polarization of the optical waves throughout the interaction length.

Assuming that in the geometry illustrated in Fig.2 the incident optical wave is linearly polarized with electric field lying in the xy plane the effective photoelastic constant for a BCAOI which involves longitudinal acoustic wave in optically isotropic materials is

$$p_{eff} = p_{12} \qquad (6)$$

From Ref.[9] one obtains p_{12} = 0.271 for FS at 0.6328 μm while for Ge at 10.6 μm p_{12} = 0.235. Using the longitudinal acoustic velocity given in Table 1 and expression (5) the following figures of merit are obtained

$$M = 15.24 \times 10^{-16} \ (S^3/k_g) \text{ for FS at } 0.6328\ \mu m$$

$$M = 3.53 \times 10^{-13} \ (S^3/k_g) \text{ for Ge at } 10.6\ \mu m$$

In Eqn.(7b) the arbitrarily chosen propagation direction of the longitudinal acoustic waves is along [100] axis of the Ge single crystal.

It is noted that these high figures of merit make BCAOI attractive from the point of view of acoustic power level required to obtain a certain diffraction efficiency. Moreover BCAOI exhibits the feature that the phase matching requirement, Bragg condition, is to, first order, not sensitive to small change of the orientation of optical waves and hence may be of interest for implementing acousto-optic tunable filters.

For the above two materials the acoustic frequency and the optical wavelength shifts predicted by Eqns. (1) and (2) were calculated. Results are presented in Table 2. This Table also includes three common uniaxial crystals which are considered below.

Table 2 ACOUSTIC PROPERTIES AT $k_a = 2\ k_o$

MATERIAL	ACOUST. FREQ. (GHz) at λ_o	DISTANCE $100\ \lambda_a$ (μm)	ATTEN. $100\ \lambda_a$ (db)	TRANSIT TIME $100\ \lambda_a$ (ns)
Fused Silica	13.21 (1.31 μm)	44.9	9.41	7.57
Ge [1 0 0]	3.72 (10.6 μm)	132.5	5.50	26.91
$LiNbO_3$ [1 0 0]	23.08 (1.31 μm)	28.5	0.23	4.33
Quartz [0 0 1]	14.98 (1.31 μm)	42.4	2.00	6.68
TeO_2 [0 0 1]	10.51 (1.31 μm)	29.9	4.81	9.51

2.1.2 Uniaxial crystals

Three uniaxial single crystals listed in Tables 1 and 2 are considered as substrates for BCAOI. Two types of configurations are considered namely, (i) those in which the optical and acoustic wavevectors are orthogonal to the optical axis as shown in Fig.3 and (ii) configurations in which both wavevectors lie in a plane which is arbitrarily oriented with respect to the optical axis. The wavevector diagram for the later configuration is shown in Fig.4 [10]. Such configuration exhibits a wide angular aperature irrespective of the crystal being positive or negative uniaxial crystals. In uniaxial crystals BCAOI can take place when the acoustic wave is either longitudinal or shear. Since only longitudinal transducers have been demonstrated at very high frequency experimentally, BCAOI which involves longitudinal acoustic waves are mainly

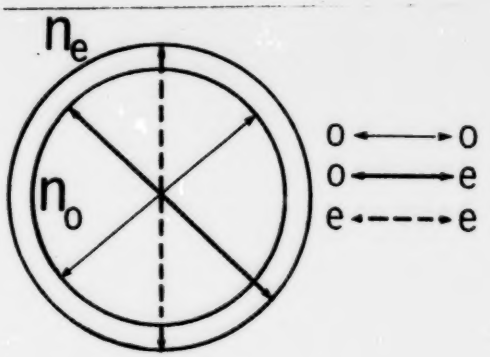

Fig.3 BCAOI in positive uniaxial crystals whose optical and acoustic wavevectors are orthogonal to the optical axis. For negative crystals n_e and n_o are interchanged.

considered here. However, one example of BCAOI with shear acoustic waves is also given below.

Using Eqn.(1) one obtains the following acoustic frequencies for the configurations shown in Fig.3; (i) $f_a = v_a/\lambda_o\ (n_o + n_e)$: when the incident and diffracted waves have different polarization, (ii) $f_a = (v_a/\lambda_o)2n_o$: when both waves are ordinary and (iii) $f_a = (v_a/\lambda_o)2n_e$: when both waves are extraordinary, where v_a can be longitudinal or shear acoustic wave velocity. For illustration purposes only figures of merit of BCAOI in lithium nicbate single crystal are calculated. The results are given in Table 3. For acoustic waves propagating along the [100] direction of lithium niobate only the longitudinal mode yields BCAOI. The p_{eff} and the corresponding M for configuration in Fig.3 are given in Table 3. BCAOI in lithium niobate which involves shear mode can be obtained, for example, using [1 0 0] polarized, [0 1 0] propagating wave; The corresponding p_{eff} is $p_{41} = -0.151$. Taking into acount the high M value in the last row of Table 3 and low acoustic attenuation in Table 1, acousto-optic devices using BCAOI in lithium niobate may be attractive.

Table 3 BCAOI p_{eff} and FIGURES OF MERIT IN LITHIUM NIOBATE FOR LONGITUDINAL ACOUSTIC WAVE ALONG [100]

INTERACTION	p_{eff}	$M \times 10^{-16}\ (S^3/k_g)$
ord. to ext.	-0.151	22.38
ord. to ord.	0.090	8.98
ext. to ext.	0.179	31.45

(ord.: ordinary; ext.: extraordinary)

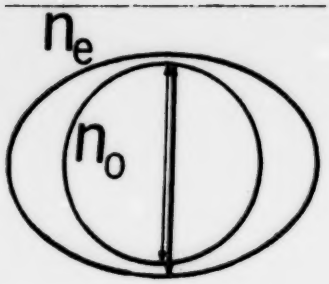

Fig.4 BCAOI in positive uniaxial crystals whose optical amd acoustic wavevectors lie in a plane which is arbitrarily oriented with respect to the optical axis.

Another configuration of interest is that in which the optical axis is off-set from the interaction plane, the optical wavevector loci for the ordinary and extraordinary polarized waves are illustrated in Fig.4 [10]. The "gap" between the loci allows us to implement a BCAOI involving, for instance, an ordinary wave which is coupled into an extraordinary wave. The required frequency for such interactions as a function of θ, the offset angle, which is given here for the first time, is

$$f_a = \frac{v_a}{\lambda_o}\left[\frac{n_o n_e}{(n_o^2 \cos^2\theta + n_e^2 \sin^2\theta)^{1/2}} + 1\right] \quad (7)$$

and that for an ordinary to an ordinary BCAOI is given by $f_a = (v_a/\lambda_o)2n_o$. By substracting this expression from Eqn. (7) one obtains

$$\Delta f_a = \frac{v_a}{\lambda_o}\left[\frac{n_o n_e}{(n_o^2 \cos^2\theta + n_e^2 \sin^2\theta)^{1/2}} - 1\right] \quad (8)$$

By properly choosing "θ" one can make Δf_a small enough to fall within the acoustic transducer bandwidth. It means that the diffracted light may be controlled to have ordinary or extra-ordinary polarizations by changing the acoustic frequency.

2.2 CONSIDERATIONS OF ACOUSTIC PROPAGATION LOSS

The strength of BCAOI is in general proportional to the interaction length normalized by the acoustic wavelength λ_a (= v_a/f_a). Since the acoustic attenuation normally increases as a function of f_a^2, therefore the interaction strength deteriorates as the acoustic frequency increases. In this section only longitudinal acoustic waves are considered.

Table 1 lists the material properties of some common materials for acousto-optic interactions [9]. n is the optical refractive index, whereas subscripts o and e denote the ordinary and extra-ordinary waves respectively. Under the condition of k_a equal to $2k_o$, the corresponding acoustic frequency, acoustic propagation distance, loss (α) and time delay across a length of 100 acoustic (longitudinal wave) wavelengths in these materials for optical ordinary waves only are given in Table 2. It means that in Table 2, k_o is equal to $2\pi n_o/\lambda_o$. Optical wavelength 1.31 μm is chosen because it is currently used in single mode optical fiber telecommunications. Since Ge is optical transparent around CO_2 laser wavelength but not the other materials listed in Table 1, 10.6 μm is selected for Ge only. It can be seen that the loss may be tolerable for some of the practical acousto-optical device appications. The one-way tuned loss for a multilayer zinc oxide thin film transducer on a sapphire substrate has been reported to be 17 dB at around 12 GHz and room temperature [5]. This transducer loss may be improved further [5,6,7].

2.3 SUMMARIES

The merits of BCAOI can be summerized as below:

A. There is no "forbidden" BCAOI configuration in any isotropic, uniaxial or biaxial material having low acoustic and optical loss.

B. Incident light with ordinary or extra-ordinary polarization may be coupled into diffracted light with ordinary, extraordinary or both polarizations by proper choices of crystal orientations.

C. By a proper choice of crystal orientations there may exist a very small gap between the loci of the ordinary and the extra-ordinary optical waves. It means that within the bandwidth of the acoustic transducer the diffracted light can be controlled to have ordinary or extra-ordinary polarizations by changing the acoustic frequency. In general this particular direction also has very large optical aperture. One possible application is that there may exist a direction that the coupling strength to the ordinary and the extraordinary are equal.

3. BCAOI IN SINGLE MODE FIBERS

In-line fiber-optic signal processing devices which may be simple, small size and inexpensive can process guided light directly within the optical fiber [11-13]. Acousto-optic interactions performed directly with the guided optical waves in optical fibers have been demonstrated using symmetric standing bulk acoustic waves, propagating bulk [12], surface [11] and flexural [13]

acoustic waves as well as thermal excited phonons (Stimulated Brillouin phenomenon) [14,15]]. Fiber-optic phase modulators, frequency shifters, amplitude modulators, switches and filters may be achieved by these devices and potentially used in the fiber optic telecommunication and sensor field.

Stimulated Brillouin scattering phenomena in single mode optical fibers have been also reported, but only a few involving backward scattering (SBBS) are cited here [14-17]. SBBS is also an acousto-optic phenomenon, but acoustic waves are generated by the heat induced by the guided light inside the fiber core rather than the ultrasonic transducers. For SBBS a nearly infinite number of acoustic modes exist and many are responsible for the light scattering, thus it is difficult to select the frequency of the guided acoustic waves. Long length of fiber is also required to achieve the required efficiency. It is noted that SBBS is one of the main factors which limit the maximum transmittable optical energy guided in the core of a single mode fiber, and also it is one the considerations in the design of an optical fiber system employing frequency-division multiplexing scheme and gain-introduced transmission lines utilizing SBS.

In this section a theoretical analysis for backward collinear guided-wave acousto-optic interactions (BCAOI) inside the fiber core of a single mode fiber been believed to be responsible for the experimental observation of SBBS reported in Ref.[16]. Furthermore, the high frequency ultrasonic transducers (> 10 GHz) have been demonstrated recently [13,14]. It means that the high frequency acoustic waves for the BCAOI inside a single mode cladded fiber may be excited directly by an ultrasonic transducer. Figure 5 shows a considered geometry with the ultrasonic transducer attached to the fiber end. Practical considerations will be discussed.

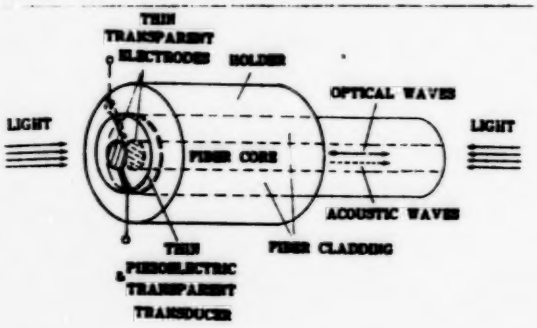

Fig.5 A geometry of the device consisting of an ultrasonic transducer bonded to the te mination of a cladded fiber in which guided acoustic and optical waves can propagate simultaneously with low loss and low dispersion.

3.1 ANALYSIS

In the analysis for BCAOI in single mode fibers, fibers are assumed to satisfy the weakly guiding conditions for both optical [18] and acoustic waves [19,20]. It means that the phase velocity in the fiber core is slightly smaller than that in the fiber cladding. The geometry considered in the present study is given in Fig.5. An ultrasonic transducer is attached to the termination of a cladded fiber in which both single mode optical and acoustic waves propagate inside the fiber core. The electrodes of this transducer can be either transparent or reflective. The acoustic waves are launched into the fiber through the ultrasonic transducer which determines the desired propagating acoustic mode. The guided optical waves are launched from a light source.

When guided acoustic waves propagate inside the fiber core, they produce a periodic modulation of the optical refractive index via the elasto-optical effect. This provides a spatial grating for the guided optical waves. Then BCAOI takes place by converting the single guided optical mode (LP_{01} or HE_{11}) propagating in the forward (say +z) direction to the same optical mode but propagating in the backward (-z) direction due to the high frequency travelling acoustic wave in the z or -z direction with k_a equal to $2k_o$, where k_a and k_o are the acoustic and optical wavenumbers respectively. Under such condition the diameter of the fiber core is about a few or tens acoustic wavelengths. A cladded fiber may be also designed to be able to guide both optical and acoustic waves in single mode operation inside the fiber core [21].

3.1.1 Dispersion Equations for Single Mode Operation

Under weak guidance conditions the dispersion equation for the single optical mode (LP_{01}) [18], single shear (F_{11}) [19] and longitudinal (L_{01}) [20] acoustic mode can be approximated expressed in an identical mathematical form as follows [21]

$$\frac{J_0(U)}{U\,J_1(U)} - \frac{K_0(W)}{W\,K_1(W)} = 0 \qquad (9)$$

where J and K are Bessel and modified Bessel functions respectively, and

$$U = \omega a\left(\frac{1}{v_1^2} - \frac{1}{v^2}\right)^{1/2} \qquad (10)$$

$$W = \omega a\left(\frac{1}{v_2^2} - \frac{1}{v_2^2}\right)^{1/2} \qquad (11)$$

$$V = \omega a\left(\frac{1}{v_2^2} - \frac{1}{v_1^2}\right)^{1/2} \qquad (12)$$

where a is the core radius; v_1 and v_2 are the phase velocity of the core and cladding materials respectively. For opitcal LP_{01} mode $v_1 = C/n_1$ and $v_2 = C/n_2$, where n is the refractive index. For acoustic F_{11} mode, $v_1 = v_{S1}$ and $v_2 = v_{S2}$ and for L_{01} mode $v_1 = v_{L1}$ and $v_2 = v_{L2}$. $\omega = 2\pi f$ where f is the frequency.

V is a normalized frequency which has no dimension [18,21]. If V is less than 2.405 the fiber is operated in the single mode regime. The dispersion curves for a few lower order modes are given in Fig.6. Field distributions of these modes can be found in Refs.[18-20].

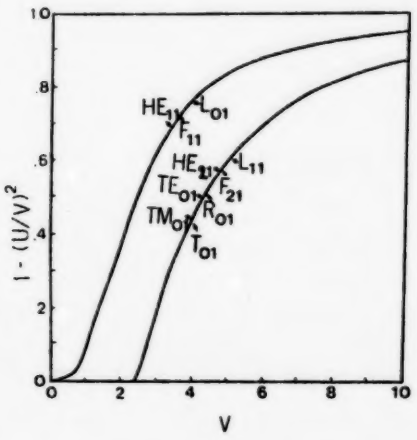

Fig.6 The dispersion curves of a few lower order guided optical and acoustic modes in weakly guiding fibers. The guided modes are hybrid (HE or EH), transverse electrical (TE_{nm}) or transverse magnetic optical modes (TM_{nm}), and flexural or shear (F_{nm}), tortional (T_{nm}), radial-axial (R_{nm}) and longitudial (L_{nm}) modes

3.1.2 BCAOI

Although only longitudinal wave transducers at very high frequency was demonstrated experimentally [5,6], efficicent shear wave transducers have been predicted theorectically [7]. Thus in this section the lowest order longitudinal L_{01} mode and shear F_{11} mode are selected for the analysis.

If the ultrasonic transducer in Fig.1 is a longitudinal or shear type, then L_{01} or F_{11} acoustic mode may be efficiently excited respectively. It is noted that many guided acoustic modes can be generated in the SBBS measurement in single mode optical fibers [14-17].

3.1.3 Selection of Fiber Parameters

Since the acoustic frequency required for the BCAOI is very high, the dopants such as GeO_2 in doped fused silica act like inhomogeneities and induce higher optical and acoustic loss. In order to reduce such a loss pure fused silica is preferrable as the core material and thus it is used here for the calculation. The assumed core radius and the operating optical wavelength of the single mode optical fiber is 3 and 1.31 μm respectively [22].

Equation (12) can be rewritten as

$$V = k_o a \delta_o = k_o a\,[1-(n_2/n_1)^2]^{1/2} \qquad (13)$$

for the guided optical waves;

$$V = k_a a \delta_a = k_a a\,[1-(v_{L2}/v_{L1})^2]^{1/2} \qquad (14)$$

for the guided longitudinal accustic waves.

$$V = k_a a \delta_a = k_a a\,[1-(v_{S2}/v_{S1})^2]^{1/2} \qquad (15)$$

for the guided shear acoustic waves.

At 1.31 μm optical wavelength, n_1 of the pure fused silica is equal to 1.4465 extrapolated from the data in Ref.[23]. Let V_o for the guided LP_{01} mode be 2.405. From Eqn.(13) we obtain n_2 = 1.4367. The density (ρ), longitudinal (v_L) and shear wave velocity (v_S) for fused silica is 2202 kg/m^3, 5933 m/s and 3764 m/s respectively [20]. In order to meet the criterion $k_a = 2k_o$ for longitudinal

or shear acoustic waves, from Eqns.(13)&(14) and Eqns.(13)&(15) v_{L2} and v_{S2} are then equal to $1.0068\,v_{L1}$ and $1.0068\,v_{S1}$ respectively.

3.2 Formulations of Coupling Coefficients

Diffraction of guided optical waves due to guided acoustic waves can be described by the coupling equation [8]

$$\frac{dA_i(z)}{dz} = -j\,C^{*}(z)\,A_d(z)\,e^{-j2\delta z} \tag{16}$$

$$-\frac{dA_d(z)}{dz} = -j\,C(z)\,A_i(z)\,e^{j2\delta z} \tag{17}$$

where A_i and A_d are the amplitudes of incident and diffracted optical waves, respectively and z is the distance along the longitudinal axis of the fiber shown in Fig.5; 2δ is the shift from the Bragg condition given by Eq.(1) and is written as

$$2\delta = -k_{od} - k_{oi} + k_a . \tag{18}$$

The coupling coefficient C(z) is generally a function of distance z along the longitudinal axis of the fiber. The superscript * denotes the complex conjugate. In this study the acoustic wave propagation loss in the BCAOI region is assumed to be negligible, thus C(z) is independent of z. The coupling efficiency simplified under the condition of $\delta = 0$ is

$$\eta = \tanh^2(|C|L) \tag{19}$$

The coupling coefficient C is represented by a summation

$$C = C^{t} + C^{z} + C^{rz} + C^{r\phi} + C^{\phi z} \tag{20}$$

C^{t} and C^{z} are the coupling coefficients for optical transverse and longitudinal components, respectively, and are given by

$$C^{t} = \frac{\omega_o \epsilon_0}{4} \iint \left(E_r^{*}\,\Delta\epsilon_{rr}\,E_r + E_\phi^{*}\,\Delta\epsilon_{\phi\phi}\,E_\phi \right) r\,dr\,d\phi \tag{21a}$$

$$C^{z} = \frac{\omega_o \epsilon_0}{4} \iint E_z^{*}\,\Delta\epsilon_{zz}\,E_z\,r\,dr\,d\phi \tag{21b}$$

where ω_o is the optical angular frequency and ϵ_0 is the dielectric constant of free space. The diagonal and off-diagonal components of dielectric perturbations are induced by acoustic strains S_{ij} through photoelastic constants p_{ij} as

$$\Delta\epsilon_{rr} = -n^4(r)\left[p_{11}(r)S_{rr} + p_{12}(r)S_{\phi\phi} + p_{12}(r)S_{zz}\right] \tag{22a}$$

$$\Delta\epsilon_{\phi\phi} = -n^4(r)\left[p_{12}(r)S_{rr} + p_{11}(r)S_{\phi\phi} + p_{12}(r)S_{zz}\right] \tag{22b}$$

$$\Delta\epsilon_{zz} = -n^4(r)\left[p_{12}(r)S_{rr} + p_{12}(r)S_{\phi\phi} + p_{11}(r)S_{zz}\right] \tag{22c}$$

$$\Delta\epsilon_{rz} = -2n^4(r)p_{44}(r)\,S_{rz} \tag{22d}$$

$$\Delta\epsilon_{r\phi} = -2n^4(r)p_{44}(r)\,S_{r\phi} \tag{22e}$$

$$\Delta\epsilon_{\phi z} = -2n^4(r)p_{44}(r)\,S_{\phi z} \tag{22f}$$

The off-diagonal $\Delta\epsilon$'s given in Eqns.(22d)-(22f) induce the coupling coefficients C^{rz}, $C^{r\phi}$ and $C^{\phi z}$ between optical transverse and longitudinal components as given by Eqns.(23a)-(23c) respectively

$$C^{rz} = \frac{\omega_o \epsilon_0}{4} \iint E_z^{*}\,\Delta\epsilon_{rz}\,E_r\,r\,dr\,d\phi \tag{23a}$$

$$C^{r\phi} = \frac{\omega_o \epsilon_0}{4} \iint E_r^{*}\,\Delta\epsilon_{r\phi}\,E_\phi\,r\,dr\,d\phi \tag{23b}$$

$$C^{\phi z} = \frac{\omega_o \epsilon_0}{4} \iint E_\phi^{*}\,\Delta\epsilon_{\phi z}\,E_z\,r\,dr\,d\phi \tag{23c}$$

The detailed analytical expressions of the strain components and coupling coefficients for both Longitudinal L_{01} and shear F_{11} modes are very lengthy. They will be presented elsewhere. Here, only the numerical results are to be given in the next section.

3.3 Numerical Calculation of the Coupling Coefficient

The coupling coefficient of the BCAOI in single mode optical fiber discussed in section 3.2 are evaluated here.

3.3.1 Coupling Coefficient for L_{01} Mode

Figure 7 shows the coupling coefficient C calculated for longitudinal L_{01} mode as a function of V-value of acoustic waves, V_a, where a constant v_{L1} value of 5933 m/s is

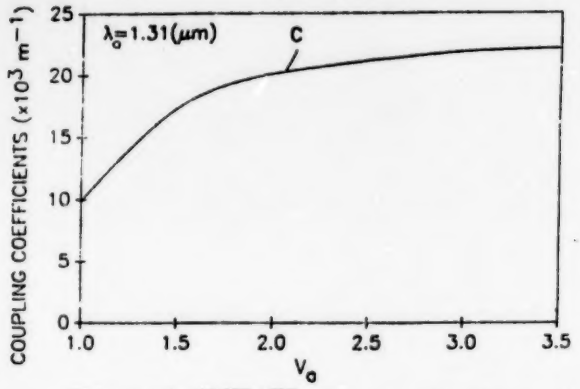

Fig.7 Coupling coefficient C as a function of V_a.

assumed and the value v_{L2} is varied to change V_a. The photoelastic constants are assumed to be the value of vitreous silica at λ_o=0.6328 μm as p_{11}=0.121, p_{12}=0.271 and p_{44}=-0.075 for the core and cladding materials. The calculated coupling coefficients C_{rz}, $C_{r\phi}$ and $C_{\phi z}$ between optical transverse and longitudinal components are negligible comparing C_t and C_z, therefore only two dominant components are shown. In Fig.7 the ratio of the coupling coefficients C_t which is the most dominant for L_{01} mode between the core and cladding are also shown. This ratio increases with the increase of V_a, because the acoustic power concentrates more in the core region with the increase of V_a.

The dependence of the coupling coefficient on the optical wavelength is calculated as shown in Fig.8(a), where the acoustic properties of the fiber are assumed to be v_{L1}=5933.0 m/s, v_{L2}=5943.0 m/s, v_{S1}=3764.0 m/s, v_{S2}=3770.3 m/s and ρ = 2202 kg/m³. As the wavelength dispersion of refractive index in the fiber, the gradient $dn(\lambda_o)/d\lambda_o$ of a fused silica [24] was assumed for both core and cladding materials. The photoelastic constants were assumed to be independent of the wavelength. The acoustic frequency satisfying Eqn.(2) is plotted as well as acoustic and optical V-values in Fig.8(b). The V-values in acoustic and optical waves are the same. The coupling coefficient C_t in

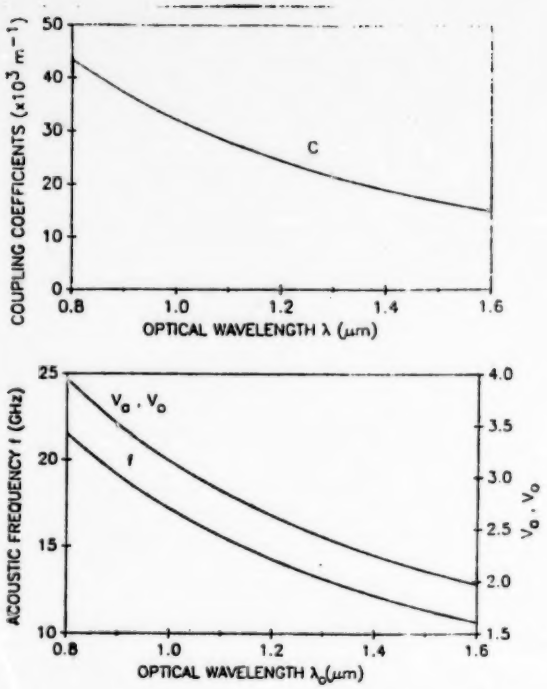

Fig.8 (a) Dependence of the coupling coefficient on the optical wavelength, , and (b) the normalized acoustic ,V_a and optical, V_o, frequencies and the acoustic frequency, f, required for the BCAOI

the core increases with the decrease of the wavelength because both optical and acoustic power concentrate more in the core region. The total coupling coefficient also increases with the decrease of the wavelength. However, it is noted that the fiber becomes multimode when the V-value exceeds 2.405.

Now, consider the coupling efficiency using Eqn.(19). The coupling coefficient C is 2.12×10^{4} m^{-1} when the acoustic power is equal to 1 watt. This coupling coefficient is proportional to a square root of acoustic power. Suppose the coupling length L be 100 Λ, which corresponds to a total distance of 45.4 μm, where Λ is the acoustic wavelength. Then, the coupling efficiency is 55.6 % and 8.7 % when the acoustic power is 1 watt and 0.1 watt, respectively. If the coupling length can be 1000Λ, the coupling efficiency increases to 99.1 % and 55.6 % with acoustic power of 0.1 watt and 0.01 watt, respectively.

3.3.2 Coupling Coefficient for F_{11} Mode

In our calculations it is found out that BCAOI can only exist for guided longitudinal modes, L_{0m} and L_{2m}, and shear modes, F_{2m},

and radial-axial modes, R_{0m} ; m= 1, 2, 3.... This can be seen by considering the overlap integral of the electromagnetic field of the HE_{11} mode and the displacement profile of the guided acoustic modes. Therefore there is no coupling for BCAOI between the HE_{11} mode and the lowest order shear acoustic mode, F_{11}.

3.4 SUMMARIES

The theoretical analysis for BCAOI in a weakly guiding single mode fiber was presented. This interaction is believed to be responsible for the experimental observation of SBBS phenomena reported in Ref.[15,16]. SBBS is one of the important factors which limit the maximum transmittable optical energy in a single mode optical fiber communication network. As a result of recent progress on very high frequency piezoelectric transducers [6-8] which can be grown at the fiber end surface, in-line fiber-optic frequency shifters, tunable filters, switches, amplitude modulators, etc empolying BCAOI may be constructed.

Future research will also include BCAOI in cladded single crystal fibers which have much lower acoustic loss and larger optical dispersion. The lower acoustic loss enhances the effective BCAOI length thus the coupling efficiency, and the higher optical dispersion narrows the optical filter bandwidth.

ACKNOWLEDGEMENTS

The authors would like to thank Dr. N. Goto for his helpful discussions.The research support partially from the Natural Sciences and Engineering Research Council of Canada is acknowledged.

REFERENCES

[1] S.E. Harris and R.W. Wallace, "Acousto-optic tunable filter", J. Opt. Soc. Am., 59, 774-747 (1969).
[2] R.W. Dixon, "Acoustic diffraction of light in anisotropic media", IEEE J. Quantum Electron., QE-3, 85-93 (1967).
[3] I.C. Chang, "Acoustooptic devices and applications", IEEE Trans. Sonics and Ultrason., SU-23, 2-22 (1976).
[4] J.B. Houston, M. Gottlieb, S.K. Yao, I.C. Chang, J. Tracy, L.M. Smithline and G.J. Wolga, "The potential for acousto-optics in Instrumentation: an overview for the 1980's", Opt. Eng., 20, 712-718 (1981)
[5] B. Hadimioglu, B.T. Khuri-Yakub, L.C. Goddard and C.F. Quate, "Multi-layer ZnO acoustic transducers", Proc. IEEE Ultrasonics Symp., 361-364 (1986)
[6] B. Hadimioglu, L.J. La Comb, Jr., D.R. Wright, B.T. Khuri-Yakub and C.F. Quate, "High efficiency, multiple layer ZnO acoustic transducers at millimeter wave frequencies", Appl. Phys. Lett., 50, 1642-1644 (1987).
[7] E. Akcakaya, E.L. Adler and G.W. Farnell, "Anisotropic superlattice transducers: characteristics and models", to be presented in Ultrasonics Symp. Chicago, Ill. Oct. 1988.
[8] A. Yariv and M. Nakamura, "Periodic structures for integrated optics", IEEE J. Quantum Electron., QE-13, 233-253 (1977).
[9] Data were collected from many references but mainly from: N. Uchida and N. Niizeki, "Acoustooptic deflection materials and techniques", Proc.IEEE, 61, 1073-1092 (1973).
[10] J.E.B. Oliveira and E.L. Adler, 'Analysis of off-optical axis anisotropic diffraction in tellurium at 10.6 μm', IEEE Trans. Ultrasonics, Ferroelectrics and Freq. Contr l, UFFC-34, 86-92 (1987).
[11] ..P. Risk, G.S. Kino, H.J. Shaw and R.C. Youngquist, "Acoustic fiber-optic modulators" Proc. IEEE Ultrasonics Symp., 318-327 (1984).
[12] S.S. Tarng and I.C. Chang, "High frequency Acousto-optic modulation in single mode fiber", Proc. IEEE Ultrasonic Symp., 429-431 (1985).
[13] B.Y. Kim, J.N. Blake, H.E. Engan and H.J. Shaw, "All-fiber acousto-optic frequency shifter", Opt. Lett., 11, 389-391 (1987).
[14] P.J. Thomas, N.L. Rowell, H.M. van Driel and G.I. Stegeman, "Normal acoustic modes and Brillouin scattering in single mode optical fibers", Phys. Rev. B, 19, 4986-4998 (1979).
[15] B.W. Tkach, A.R. Chraplyvy and R.M. Derosier, "Spontaneous Brillouin scattering for single mode optical fiber characterisation", Electron. Lett., 22, 1011-1013 (1986).
[16] N. Shibata, Y.Azuma, T. Horiguchi and M. Tateda, "Identification of longitudinal acoustic modes guided in the core region of a single-mode optical fiber by Brillouin gain spectra measurements", Opt. Lett., 13, 595-597 (1988).
[17] R.M. Shelby, M.D. Levenson and P.W. Bayer, "Guided acoustic-wave Brillouin scattering", Phys. Rev. B. 31, 5244-5252 (1985).
[18] D. Gloge, "Weakly guiding fibers", Appl. Opt., 10, 2252-2258 (1971).
[19] A. Safaai-Jazi, C.K. Jen and G.W. Farnell: 'Analysis of weakly guiding fiber acoustic waveguides', IEEE Trans. on Ultrasonics, Ferroelectrics and Frequency Control, SFFC-33, 59-68 (1986).
[20] C.K. Jen, A. Safaai-Jazi and G.W. Farnell: 'Leaky modes in weakly guiding fiber acoustic waveguides', IEEE Trans. on Ultrasonics, Ferroelectrics and Frequency Control, UFFC-33, 634-643 (1986).
[21] C.K. Jen, "Similarity and differences between fiber acoustics and fiber optics", Proc. of IEEE Ultrasonics Symp., 1128-1133 (1985).
[22] For example, "Optical fiber technology", D. Gloge ed., IEEE Press, N.Y. 1976 and "Optical fiber technology II", C.K. Kao ed., IEEE Press, New York, 1981.
[23] S. Kobayashi, "Refractive index dispersion of doped fused silica", IOOC, 309-312 (1977).
[24] Handbook of optical constants of solids, Edited by E. D. Palik, Academic Press, Orlando, 1985.